hexagonal;[18,19] K_2OsCl_6 and K_2OsBr_6 are cubic with K_2PtCl_6 structure.[20] The Os–Cl distance in K_2OsCl_6 is 2.36 Å compared with our determined value of 2.332 Å (av). Assuming as before an ionic radius of Cl^- of 1.81 Å, the radius of Os(IV) becomes 0.52 Å. In spite of the low (triclinic) crystal symmetry, the $OsCl_6^{2-}$ octahedron is almost undistorted. Another related structure is that of $OsCl_4$,[21] which contains endless chains of linked $OsCl_6$ octahedra. In this structure the terminal Os–Cl distance is 2.262 Å and the bridging Os–Cl is 2.378 Å, with a weighted average Os–Cl distance of 2.339 Å.

It is of interest to note that the dihedral angles, i.e., the angles of rotation of the phenyl groups in $(C_6H_5)_4P^+$ out of the appropriate C(4)–C(1)–P–C(1)′–C(4)′ plane, have totally differing values of 1°, 37°, 71°, and 88°. The corresponding value in I is 54°. The energy barrier to rotation of these groups must be exceedingly low since the ring can clearly adopt any rotational angle from almost parallel to almost perpendicular to the carbon–phosphorus plane, depending upon influences from the environment. In the structure of $(C_6H_5)_4PI$,[13] the experimental value for the dihedral angle is 62°, and it is claimed that the optimum value for minimum steric hindrance is 38°. In two other papers,[12,14] the dihedral angles are not given at all, but from a figure in ref 14 on $[(C_6H_5)_4P]CuCl_3$ it would seem that two of them are almost 0° and two close to 90°, again indicating the variability of these angles.

Registry No. I, 86365-50-6; II, 86392-81-6.

Supplementary Material Available: Tables of observed and calculated structure factors and thermal parameters for compounds I and II (27 pages). Ordering information is given on any current masthead page.

(18) Hepworth, M. A.; Robinson P. L.; Westland, G. J. *J. Chem. Soc.* **1958**, 611.
(19) Brown, D. H.; Dixon, K. R.; Kemmitt, R. D. W.; Sharp, D. W. A. *J. Chem. Soc.* **1965**, 1559.
(20) McCullough, J. D. *Z. Kristallogr.* **1936**, *94*, 143.
(21) Cotton, F. A.; Rice, C. E. *Inorg. Chem.* **1977**, *16*, 1865.

Contribution from the Departments of Chemistry, University of Illinois, Urbana, Illinois 61801, and State University of New York at Buffalo, Buffalo, New York 14214

Synthesis, Characterization, and Reversible Photochemical/Thermal Interconversion of η^1- and η^2-Bridged (Aryldiazo)triosmium Clusters. Crystal Structure of $(\mu\text{-H})Os_3(CO)_{10}(\mu\text{-}\eta^2\text{-N=NPh})$[1]

DEBORAH E. SAMKOFF,[†] JOHN R. SHAPLEY,*[†] MELVYN ROWEN CHURCHILL,*[‡]
and HARVEY J. WASSERMAN[‡]

Received January 11, 1983

$H_2Os_3(CO)_{10}$ reacts with $ArN_2^+BF_4^-$ (Ar = Ph, $p\text{-}C_6H_4F$, $p\text{-}C_6H_4CH_3$) in refluxing dichloromethane to produce, after neutralization, the compounds $HOs_3(CO)_{10}(N_2Ar)$ (**1**), in which the aryldiazo ligand bridges one edge of the osmium triangle through one nitrogen atom. UV photolyses of **1** produce the isomeric series of compounds **2**, in which the aryldiazo ligand bridges one edge of the osmium triangle through both nitrogen atoms. This isomerization is reversible thermally. Quantum yields for the photoisomerization at 313 and 366 nm, 0.06 and 0.006, respectively, indicate that higher energy light is more efficient at causing the transformation. The structure of $(\mu\text{-H})Os_3(CO)_{10}(\mu\text{-}\eta^1\text{-N=N-}p\text{-}C_6H_4CH_3)$ has been previously determined by a single-crystal X-ray diffraction study. The results of a crystallographic study on $(\mu\text{-H})Os_3(CO)_{10}(\mu\text{-}\eta^2\text{-N=Ph})$ are reported herein. This complex crystallizes in the noncentrosymmetric orthorhombic space group $P2_12_12_1$ with $a = 9.482$ (2) Å, $b = 12.542$ (3) Å, $c = 17.588$ (4) Å, $V = 2091.6$ (7) Å^3, and $Z = 4$. The structure was solved by a combination of Patterson, difference-Fourier, and full-matrix least-squares refinement. All non-hydrogen atoms were located; final discrepancy indices are $R_F = 7.7\%$ and $R_{wF} = 7.4\%$ for all 2114 independent data. The $(\mu\text{-}\eta^2\text{-N=NPh})$ ligand spans the Os(2)–Os(3) linkage, with Os(3)–N(1) R_F 2.14 (2) Å, Os(2)–N(2) = 2.11 (3) Å, and N(1)–N(2) = 1.20 (4) Å. The (μ-hydrido, μ-aryldiazo) dibridged Os(2)–Os(3) distance is 2.895 (2) Å as compared to Os(1)–Os(2) = 2.868 (2) Å and Os(1)–Os(3) = 2.862 (2) Å.

Introduction

Mononuclear aryldiazo (N_2Ar) complexes may have the $M\text{-}N_\alpha\text{-}N_\beta$ group bent at N_β only (I) or at both N_α and N_β (II).[2–6] In the former case, the neutral ligand is a 3-electron

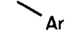

I

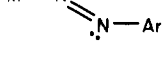

II

donor to the metal; in the latter case, it is a 1-electron donor, in direct analogy with compounds of the isoelectronic nitrosyl ligand. Although many monomolecular aryldiazo complexes are known, polynuclear compounds remain rather rare. The three[7–9] structurally characterized examples have η^1-bridging aryldiazo ligands (III). Two different bridging modes (IV[10]

[†] University of Illinois.
[‡] SUNY—Buffalo.

(1) Structural Studies on Polynuclear Osmium Carbonyl Hydrides. 25. (a) Part 23: Shapley, J. R.; St. George, G. M.; Churchill, M. R.; Hollander, F. J. *Inorg. Chem.* **1982**, *21*, 3295. (b) Part 24: Churchill, M. R.; Bueno, C. *Ibid.* **1983**, *22*, 1510.
(2) Sutton, D. *Chem. Soc. Rev.* **1975**, *4*, 443.
(3) Bishop, M. W.; Butler, G.; Chatt, J.; Dilworth, J. R.; Leigh, G. J. *J. Chem. Soc., Dalton Trans.* **1979**, 1843.
(4) Hillhouse, G. L.; Haymore, B. L.; Herrmann, W. A. *Inorg. Chem.* **1979**, *18*, 2423.
(5) Schramm, K. D.; Ibers, J. A. *J. Am. Chem. Soc.* **1978**, *100*, 2932.
(6) Barrientos-Penna, C. F.; Einstein, F. W. B.; Sutton, D.; Willis, A. C. *Inorg. Chem.* **1980**, *19*, 2740.
(7) Abel, E. W.; Burton, C. A.; Churchill, M. R.; Lin, K.-K. G. *J. Chem. Soc., Chem. Commun.* **1974**, 268. Churchill, M. R.; Lin, K.-K. G. *Inorg. Chem.* **1975**, *14*, 7133.
(8) Einstein, F. W. B.; Sutton, D.; Vogel, A. L. *Inorg. Nucl. Chem. Lett.* **1975**, *12*, 671.
(9) Churchill, M. R.; Wasserman, H. J. *Inorg. Chem.* **1981**, *20*, 1580.

0020-1669/84/1323-0397$01.50/0 © 1984 American Chemical Society

and V^{11}) have been observed for complexes with *methyl*diazo ligands.

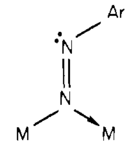

III

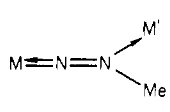

IV

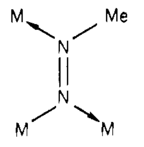

V

We now report the syntheses and reversible interconversions of $HOs_3(CO)_{10}(\mu\text{-}\eta^1\text{-}N{=}NAr)$ (**1**) and $HOs_3(CO)_{10}(\mu\text{-}\eta^2\text{-}N{=}NAr)$ (**2**) (see eq 1) and the crystal structure of $HOs_3(CO)_{10}(\mu\text{-}\eta^2\text{-}N{=}NPh)$.

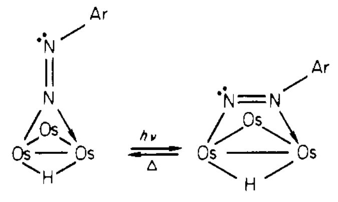

1 2 (1)

The crystal structure of $HOs_3(CO)_{10}(\mu\text{-}\eta^1\text{-}N{=}N\text{-}p\text{-}C_6H_4CH_3)$ has been reported previously.[9] $HOs_3(CO)_{10}(\mu\text{-}\eta^2\text{-}N{=}NPh)$ is, to our knowledge, the first structurally characterized example of a $\mu\text{-}\eta^2$-aryldiazo ligand.

Results and Discussion

Synthesis and Characterization of η^1 Isomers. Treatment of purple dichloromethane solutions of $H_2Os_3(CO)_{10}$ with 2- to 3-fold molar excesses of $ArN_2{}^+BF_4{}^-$ (Ar = Ph, $p\text{-}C_6H_4F$, $p\text{-}C_6H_4CH_3$) under solvent reflux results in a color change to green. When dry NH_3 is bubbled through these solutions, the green colors discharge immediately, producing yellow solutions from which compounds **1** are isolated as orange crystals. Their electron-impact mass spectra exhibit the appropriate molecular ions for $HOs_3(CO)_{10}(N_2Ar)$, as well as ions corresponding to the loss of ten carbonyl groups in each case. These compounds are air stable, both as solids and in solution. They are easily soluble in dichloromethane, chloroform, benzene, acetone, and ether and are moderately soluble in saturated hydrocarbons. Compounds **1** are unreactive toward CO, H_2, and PPh_3 under mild conditions. In hydrocarbon solution they are unreactive toward gaseous HCl. Dichloromethane solutions turn green upon treatment with HCl(g); this color change reverses moderately slowly upon standing, rapidly upon rotary evaporation of the solvent, and immediately upon treatment with dry NH_3.

The crystal structure of $HOs_3(CO)_{10}(\mu\text{-}\eta^1\text{-}N{=}N\text{-}p\text{-}C_6H_4CH_3)$ shows that the bridging, η^1-aryldiazo ligand is bent at N_β (see eq 1).[9] The $^{13}C\{^1H\}$ NMR spectrum of the same compound in solution shows ten equally intense carbonyl signals, consistent with the solid-state structure. Furthermore, the spectrum is invariant over the temperature range −55 to +55 °C, indicating that inversion of configuration at N_β is slow on this time scale.

The formation of compounds **1** is presumably initiated by adduct formation,[12] followed by hydrogen transfer first to N_β and then to ammonia (eq 2–4). Closely related chemistry has been seen in the reaction of $H_2Os_3(CO)_{10}$ with isocyanides ultimately to form $HOs_3(CO)_{10}(\mu\text{-}\eta^1\text{-}C{=}NHR)$.[13] A similar N_β-protonated intermediate has been observed in the reaction of $ArN_2{}^+$ with $(\eta^5\text{-}C_5H_5)_2WH_2$.[14,15]

$$H_2Os_3(CO)_{10} + N_2Ar^+ \rightarrow H_2Os_3(CO)_{10}(N_2Ar)^+ \quad (2)$$

$$H_2Os_3(CO)_{10}(N_2Ar)^+ \rightarrow HOs_3(CO)_{10}(N{=}NHAr)^+ \quad (3)$$

$$HOs_3(CO)_{10}(N{=}NHAr)^+ + NH_3 \rightarrow \mathbf{1} + NH_4{}^+ \quad (4)$$

Synthesis and Characterization of η^2 Isomers. Irradiation (450-W medium-pressure Hg lamp) of degassed *n*-heptane solutions of compounds **1** causes the formation of compounds **2**, which are isolated as brown crystals. At maximum conversion, the photolysis product mixture consists of ca. 85% **2** and 15% **1**. Mixtures of the same composition are obtained if pure samples of **2** are irradiated for similar periods of time. Extended photolysis, starting with either **1** or **2**, results in cluster decomposition. Pyrolyses (refluxing *n*-heptane) of solutions of **2** change their color from orange to yellow, and **1** and unreacted **2** are isolated. This reaction, at maximum conversion, yields a mixture that is >95% **1** and <5% **2** by ^1H NMR; preparative TLC of the mixture unambiguously reveals the presence of **2**. The same results are obtained by pyrolyzing solutions of pure **1** in *n*-heptane. These converisions proceed whether the atmosphere is CO, H_2, or an inert gas (N_2 or Ar); they are also unaffected by the presence of PPh_3, implying that the isomerizations are entirely intramolecular.

The compound $HOs_3(CO)_{10}(\eta^2\text{-}N{=}NPh)$ has also been prepared from the reaction of $Os_3(CO)_{10}(NCCH_3)_2$ with phenylhydrazine (see Experimental Section). The complete stoichiometry of this reaction has not been demonstrated; in particular, the fate of the two hydrogen atoms formally eliminated is unknown. Some chemistry that may be related is the reaction of $Os_3(CO)_{10}(NCCH_3)$ with triethylamine to give $HOs_3(CO)_{10}(\mu\text{-}CHCHNEt_2)$ and $H_2Os_3(CO)_{10}$.[16]

Compounds **2**, like **1**, are air stable as solids and in solution. Their electron-impact mass spectra show molecular ions for the formulations $HOs_3(CO)_{10}(N_2Ar)$, as well as ions corresponding to the loss of ten carbonyls. Compounds **2** follow the same general solubility patterns as **1**; however, for a particular aryl group compound **2** is slightly more soluble in each case than the corresponding compound **1**.

Orange dichloromethane solutions of **2** turn intensely blue upon treatment with HCl(g); this color change reverses slowly if the solutions are allowed to stand and immediately upon treatment with dry NH_3. The use of $HBF_4{\cdot}Et_2O$ results in stable blue solutions.[17] In either case, adding pentane precipitates the Cl^- or $BF_4{}^-$ salts of the protonated forms of **2**, but it has not been possible to isolate these materials in pure form. $HOs_3(CO)_{10}(\eta^2\text{-}^{15}N{=}N\text{-}p\text{-}C_6H_4CH_3)$ is fully protonated in dichloromethane with only a modest excess of $HBF_4{\cdot}Et_2O$. Under these circumstances the ^1H NMR spectrum shows a sharp doublet at δ 15.4 with $^1J^{15}NH = 81$ Hz. Both the chemical shift and coupling constant are consistent with analogous data known for aryldiazene ligands in mononuclear complexes.[18-20] In contrast, even with a large excess of added $HBF_4{\cdot}Et_2O$ (>10×), protonation of $HOs_3(CO)_{10}(\eta^1\text{-}^{15}N{=}N\text{-}p\text{-}C_6H_4CH_3)$ is not observed by

---

(10) Hillhouse, G. L.; Haymore, B. L.; Bistram, S. A.; Hermann, W. A. *Inorg. Chem.* **1983**, *22*, 314.

(11) Herrmann, W. A.; Ziegler, M. L.; Weidenhammer, K. *Angew. Chem., Int. Ed. Engl.* **1976**, *15*, 368. Weidenhammer, K.; Ziegler, M. L. *Z. Anorg. Allg. Chem.* **1979**, *457*, 174.

(12) Keister, J. B.; Shapley, J. R. *Inorg. Chem.* **1982**, *21*, 3304.

(13) Adams, R. D.; Golembeski, N. M. *J. Am. Chem. Soc.* **1979**, *101*, 2579.

(14) Carroll, J. A.; Sutton, D. *Inorg. Chem.* **1980**, *19*, 3137.

(15) Einstein, F. W. B.; Jones, T.; Hanlan, A. J. L.; Sutton, D. *Inorg. Chem.* **1982**, *21*, 2585.

(16) Shapely, J. R.; Tachikawa, M.; Churchill, M. R.; Lashewycz, R. A. *J. Organomet. Chem.* **1979**, *162*, C39. Note also the formation of $CpW(CO)_2N_2Ph$ from $CpW(CO)_3H$ and phenylhydrazine (Green, M. L. H.; Sanders, T. R.; Whiteley, R. N. *Z. Naturforsch., B: Anorg. Chem., Org. Chem., Biochem., Biophys., Biol.* **1968**, *23B*, 106) and the formal inverse of the rearrangement of $Cp_2W(H)(\eta^1\text{-}NNHPh)$ to $Cp_2W(\eta^2\text{-}NH_2NPh)$.[14]

(17) Similar intense colors are shown by the binuclear diazene complexes $[(CO)_5M]_2(\mu\text{-}NH{=}NH)$ (M = Cr, Mo, W): Sellman, D.; Brandl, A.; Endell, R. *J. Organomet. Chem.* **1975**, *97*, 229.

(18) Laing, K. R.; Robinson, S. R.; Uttley, M. F. *J. Chem. Soc., Dalton Trans.* **1975**, 839.

(19) Haymore, B. L.; Ibers, J. A. *J. Am. Chem. Soc.* **1975**, *97*, 5369.

(20) Barrientos-Penna, C. F.; Einstein, F. W. B.; Jones, T.; Sutton, D. *Inorg. Chem.* **1982**, *21*, 2578.

NMR. Thus, the basicity order ($N_\alpha > N_\beta$) observed for mononuclear doubly bent aryldiazo complexes[17,18] (see II) appears to hold also for the doubly bent ligand in compounds **1** and **2**.

Comparison of ^{15}N Chemical Shifts. The ^{15}N chemical shifts (relative to $^{15}NH_3$) determined for $HOs_3(CO)_{10}(^{15}N{=}N\text{-}p\text{-}C_6H_4CH_3)$ are δ 448.6 for isomer **1** (signal is a doublet (J = 2 Hz) due to coupling to bridging hydride), δ 693.5 for isomer **2**, and δ 319.5 (d, $^1J_{NH}$ = 81 Hz) for protonated **2**. Nitrogen atoms (sp^2 hybridized) with lone pairs localized on them resonate at parameters) low field (azobenzene occurs at δ 510.8 on the NH_3 scale); protonation results in pronounced upfield shifts in resonance positions (in the case of azobenzene, to δ 360.8).[21,22] Richards and co-workers[23] have observed the same features in the ^{15}N NMR spectra of $RhCl_2(^{15}N{=}N\text{-}p\text{-}C_6H_4NO_2)(PPh_3)_2$ (δ 707.3) and $RhCl_3(H\text{-}^{15}N{=}N\text{-}p\text{-}C_6H_4NO_2)(PPh_3)_2$ (δ 580.3). Furthermore, their results show that, for a series of mononuclear (aryldiazo)metal compounds, N_α resonates at lower field (some 200–350 ppm) if the ligand is bent also at N_α than if it is bent only at N_β. This pattern led them to propose the ^{15}N chemical shift as a criterion for deducing whether aryldiazo ligands in mononuclear compounds are singly or doubly bent. A similar distinction may result for bridging ligands, since the lone pair on N_α is coordinated in the η^1 mode but uncoordinated in the η^2 mode. This idea is consistent with the significantly lower field resonance observed for N_α in isomer **2** than in isomer **1**.

Comparison of ^{19}F NMR Shielding Parameters. ((Fluorophenyl)diazo)metal compounds may also be considered as substituted fluorobenzenes, and the electronic nature of the group consisting of the N_2 moiety, the metal, and ancillary ligands may be probed by ^{19}F NMR. Taft and co-workers[24] examined the ^{19}F chemical shifts relative to fluorobenzene (shielding parameters) of a large number of meta- and para-substituted fluorobenzenes. Of particular relevance to this discussion is their observation that, for para-substituted fluorobenzenes, a positive shielding parameter correlates with a resonance π-donor substitutent. Parshall's[25] investigation of the ^{19}F shielding parameters of $(p\text{-}C_6H_4F)PtCl(PEt_3)_2$ and $(p\text{-}C_6H_4FN{=}N)PtCl(PEt_3)_2$ showed that the substituent on the fluorobenzene is a strong resonance donor in the former case (δ 10.11) and a substantially weaker donor in the latter case (δ 2.27). The shielding parameters we have measured for $HOs_3(CO)_{10}(\eta^1\text{-}N{=}N\text{-}p\text{-}C_6H_4F)$ (δ 1.08) and $HOs_3(CO)_{10}(\eta^2\text{-}N{=}N\text{-}p\text{-}C_6H_4F)$ (δ 2.92) indicate that, as resonance donors to the ring, both triosmium diazo moieties are comparable to the platinum diazo group, with the η^2-bound diazo group a slightly stronger donor than the η^1 form.

Comparison of $\nu_{N=N}$. As part of our characterization of the isomeric ligands described in this work, we were interested in determining $\nu_{N=N}$ for the new compounds prepared during this study. The stretching frequencies of N=N double bonds are frequently near those of aryl ring modes,[26] and, in situations wher the two groups are in physical proximity (the case in aryldiazo ligands) and where coupling is symmetry allowed (likely in the cases of low molecular symmetry, such as the compounds under discussion), coupling of these vibrations makes the determinations of $\nu_{N=N}$ by inspection impossible. Haymore et al.[26] have discussed this problem and have described a technique for circumventing it, using isotopic substitution and a mathematical treatment of the resulting IR data. The N=N stretching frequencies we have extracted using their technique indicate that $\nu_{N=N}$ is more strongly dependent on the coordination mode of the aryldiazo ligand than on the electronic character of the aryl ring. In the case of the η^1 isomers, $\nu_{N=N}$ is 1525 cm^{-1}, independent of the substituent within experimental error. Due to broader absorptions in the spectra of the η^2 isomers, spectral changes accompanying isotopic substitution were more difficult to follow; however, $\nu_{N=N}$ ca. 1480 cm^{-1} is indicated for $HOs_3(CO)_{10}(\eta^2\text{-}N{=}N\text{-}p\text{-}C_6H_4CH_3)$.

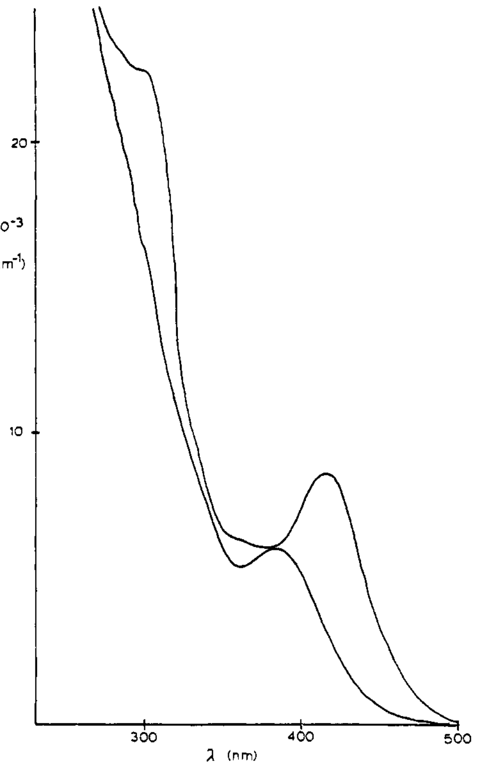

Figure 1. Electronic absorption spectra of $(\mu\text{-}H)Os_3(CO)_{10}(\eta^1\text{-}N{=}N\text{-}p\text{-}C_6H_4CH_3)$ (lower curve) and $(\mu\text{-}H)Os_3(CO)_{10}(\eta^2\text{-}N{=}N\text{-}p\text{-}C_6H_4CH_3)$ (upper curve).

Quantum Yield Determination. The electronic absorption spectra of $HOs_3(CO)_{10}(\eta^1\text{-}N{=}N\text{-}p\text{-}C_6H_4CH_3)$ and $HOs_3(CO)_{10}(\eta^2\text{-}N{=}N\text{-}p\text{-}C_6H_4CH_3)$ are displayed in Figure 1. Clearly it is the shift in the lower energy absorption that is responsible for the fact that compounds **2** are brown crystalline solids, orange in solution, while compounds **1** are orange crystalline solids, yellow in solution. It is not obvious, however, which absorption is primarily responsible for the photoisomerization. Therefore, we undertook to estimate the quantum yields for the photoisomerization at 313 nm, which is well within the higher energy absorption, and at 366 nm, which is near the 385-nm maximum of **1**. Since the extinction coefficient of **2** is everywhere greater than that of **1**, except at 385 nm, where $\epsilon(\mathbf{1}) = \epsilon(\mathbf{2})$, the quantum yields, $\phi_{313} = 0.06 \pm 0.1$ and $\phi_{366} = 0.006 \pm 0.001$, are estimates only, even at the low conversions (7 ± 2%) employed. On the other hand, greater confidence in their *relative* magnitudes is warranted, and the other-of-magnitude difference we observe is reasonable grounds for concluding that the photoisomerization results primarily from the absorption of the higher energy photons. That these quantum yields compare favorably with those reported by Gray and co-workers[27] for the reactions of $Os_3(CO)_{12}$ with CCl_4 to give $Os(CO)_4Cl_2$ ($\phi_{313} = 0.002$) and $Os_3(CO)_9(PPh_3)_3$ with PPh_3 to give $Os(CO)_3(PPh_3)_2$ (ϕ_{366} =

---

[21] Levy, G. C.; Lichter, R. L. "Nitrogen-15 Nuclear Magnetic Resonance Spectroscopy"; Wiley: New York, 1979.

[22] Duthaler, R. O.; Roberts, J. D. *J. Am. Chem. Soc.* **1978**, *100*, 4969.

[23] Dilworth, J. R.; Kan, C.-T.; Mason, J.; Richards, R. L.; Stenhouse, I. A. *J. Organomet. Chem.* **1980**, *201*, C24.

[24] Taft, R. W.; Price, E.; Fox, I. R.; Lewis, I. C.; Andersen, K. K.; Davis, G. T. *J. Am. Chem. Soc.* **1963**, *85*, 3146.

[25] (a) Parshall, G. W. *J. Am. Chem. Soc.* **1967**, *89*, 1822. (b) Parshall, G. W. *Ibid.* **1964**, *86*, 1822.

[26] Haymore, B. L.; Ibers, J. A.; Meek, D. W. *Inorg. Chem.* **1975**, *14*, 541.

[27] Tyler, D. R.; Altobelli, M.; Gray, H. B. *J. Am. Chem. Soc.* **1980**, *102*, 3022.

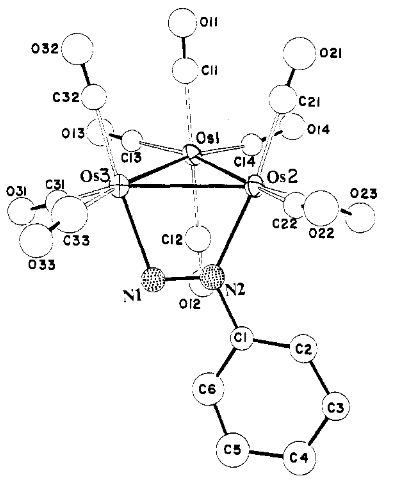

Figure 2. Molecular geometry of $(\mu\text{-H})Os_3(CO)_{10}(\mu\text{-}\eta^2\text{-N=NPh})$ (ORTEP-II diagram).

Table I. Selected Interatomic Distances (Å) for $(\mu\text{-H})Os_3(CO)_{10}(\mu\text{-}\eta^2\text{-N=NPh})$

(A) Osmium–Osmium Distances			
Os(1)–Os(2)	2.868 (2)	Os(2)–Os(3)	2.895 (2)
Os(1)–Os(3)	2.862 (2)		
(B) Osmium–Nitrogen Distances			
Os(2)–N(2)	2.11 (3)	Os(2)···N(1)	2.91 (3)
Os(3)–N(1)	2.14 (2)	Os(3)···N(2)	2.75 (3)
(C) Distances in N=NPh Ligand			
N(1)–N(2)	1.20 (4)	N(2)–C(1)	1.46 (5)
C(1)–C(2)	1.47 (5)	C(4)–C(5)	1.57 (7)
C(2)–C(3)	1.45 (6)	C(5)–C(6)	1.39 (8)
C(3)–C(4)	1.40 (7)	C(6)–C(1)	1.42 (7)
(D) Osmium–Carbonyl Distances			
Os(1)–C(11)	2.02 (5)	Os(2)–C(22)	1.97 (4)
Os(1)–C(12)	2.06 (5)	Os(2)–C(23)	1.80 (3)
Os(1)–C(13)	1.98 (4)	Os(3)–C(31)	1.89 (4)
Os(1)–C(14)	1.92 (3)	Os(3)–C(32)	2.07 (4)
Os(2)–C(21)	2.02 (6)	Os(3)–C(33)	1.88 (6)
(E) Carbon–Oxygen Distances			
C(11)–O(11)	1.13 (6)	C(22)–O(22)	1.08 (4)
C(12)–O(12)	1.03 (6)	C(23)–O(23)	1.27 (5)
C(13)–O(13)	1.11 (5)	C(31)–O(31)	1.16 (5)
C(14)–O(14)	1.15 (4)	C(32)–O(32)	1.02 (5)
C(21)–O(21)	1.00 (7)	C(33)–O(33)	1.16 (6)

Table II. Selected Interatomic Angles (deg) for $(\mu\text{-H})Os_3(CO)_{10}(\mu\text{-}\eta^2\text{-N=N-Ph})$

(A) Os–Os–Os Angles			
Os(3)–Os(1)–Os(2)	60.70 (5)	Os(2)–Os(3)–Os(1)	59.76 (5)
Os(1)–Os(2)–Os(3)	59.54 (5)		
(B) Equatorial Os–Os–C and C–Os–C Angles			
Os(2)–Os(1)–C(14)	100.1 (10)	Os(3)–Os(1)–C(13)	100.6 (10)
C(14)–Os(1)–C(13)	98.6 (15)		
Os(2)–Os(1)–C(13)	161.3 (10)	Os(3)–Os(1)–C(14)	160.7 (10)
Os(1)–Os(2)–C(23)	82.7 (12)	Os(1)–Os(3)–C(31)	85.6 (12)
C(23)–Os(2)–C(22)	104.3 (16)	C(31)–Os(3)–C(33)	98.6 (21)
C(22)–Os(2)–Os(3)	114.3 (11)	C(33)–Os(3)–Os(2)	115.4 (18)
C(23)–Os(2)–Os(3)	139.0 (12)	C(31)–Os(3)–Os(2)	139.1 (12)
(C) Trans (Diaxial) Angles			
C(11)–Os(1)–C(12)	174.5 (18)		
C(21)–Os(2)–N(2)	172.0 (16)	C(32)–Os(3)–N(1)	170.8 (13)
(D) Selected Os–Os–C (Axial) and Os–Os–N Angles			
Os(3)–Os(2)–C(21)	108.3 (15)	Os(2)–Os(3)–C(32)	105.8 (11)
Os(3)–Os(2)–N(2)	64.4 (7)	Os(2)–Os(3)–N(1)	68.6 (7)
(E) Angles at Nitrogen Atoms			
Os(3)–N(1)–N(2)	107.3 (20)	Os(2)–N(2)–C(1)	128.6 (20)
Os(2)–N(2)–N(1)	119.7 (21)	N(1)–N(2)–C(1)	111.3 (26)

Table III. X-ray Data for $(\mu\text{-H})Os_3(CO)_{10}(\mu\text{-}\eta^2\text{-N=N-Ph})$

(A) Crystal Data at 24 °C

cryst syst: orthorhombic
$V = 2091.6\ (7)$ Å^3
space group: $P2_12_12_1$ (D_2^4; No. 19)
$Z = 4$
$a = 9.482\ (2)$ Å
mol wt = 956.8
$b = 12.542\ (3)$ Å
ρ(calcd) = 3.04 g cm^{-3}
$c = 17.588\ (4)$ Å
μ(Mo Kα) = 193.2 cm^{-1}

(B) Measurement of Intensity Data

diffractometer: Syntex $P2_1$
radiation: Mo Kα ($\bar{\lambda} = 0.710\,730$ Å)
monochromator: pyrolytic graphite (equatorial mode)
scan type: coupled θ(cryst) – 2θ(counter)
2θ scan range: symmetrical, $[2.0 + \Delta(\alpha_2-\alpha_1)]°$ for $2\theta = 4–45°$
scan speed: 2.0°/min
unique data: 2114
standards: 3 mutually orthogonal reflcns collected after each batch of 97 reflcns; no significant fluctuations or decay

0.005) suggests the existence of a reasonably effective mechanism for transferring absorbed light energy from the metal–metal σ orbitals to the metal–ligand σ orbitals.

Description of the Molecular Structure of $(\mu\text{-H})Os_3(CO)_{10}(\mu\text{-}\eta^2\text{-N=NPh})$. The crystal consists of discrete molecules, separated by normal van der Waals distances. There are no abnormally short intermolecular contacts.

Figure 2 shows the labeling of atoms within the molecule, while Tables I and II, respectively, provide interatomic distances and angles. The $(\mu\text{-H})Os_3(CO)_{10}(\mu\text{-}\eta^2\text{-N=NPh})$ molecule contains a triangular triosmium core in which one osmium atom (Os(1)) is linked to four terminal carbonyl ligands; the other two osmium atoms (Os(2) and Os(3)) are each linked to three terminal carbonyl ligands, are bridged diaxially by the $\mu\text{-}\eta^2$-N=NPh ligand, and are bridged diequatorially by a hydride ligand (which was not located directly in the analysis but whose position can be deduced (see below)).

A. Deduction of Hydride Atom's Location. The position of the hydride ligand can be deduced from the following data, from arguments outlined previously[28] and on the basis of X-ray diffraction studies on the closely related species $(\mu\text{-H})Os_3(CO)_{10}(\eta\text{-}3,4\text{-}\eta^2\text{-}N_2C_3H_3)$[29] and $(\mu\text{-H})Os_3(CO)_{10}(\mu\text{-}O_2CH)$.[1a]

(1) The Os(2)–Os(3) distance of 2.895 (2) Å is lengthened relative to the distances Os(1)–Os(2) = 2.868 (2) Å and Os(1)–Os(3) = 2.862 (2) Å; the latter pair may be compared to the average value of 2.877 (3) Å found in the parent molecule $Os_3(CO)_{12}$.[30]

(2) A survey of cis-diequatorial angles around the triosmium system (Table IIIB) shows that the angles C(22)–Os(2)–Os(3) = 114.3 (11)° and C(33)–Os(3)–Os(2) = 115.4 (16)° are some 15° larger than the remaining cis-diequatorial OC–Os–Os angles (Os(2)–Os(1)–C(14) = 100.1 (10)° and Os(3)–Os(1)–C(13) = 100.6 (10)°. This effect is consistent with the presence of μ-hydride ligand (in a diequatorial site) bridging the Os(2)–Os(3) bond.

B. The Aryldiazo Ligand. This ligand occupies an η^2-bridging site with Os(3)–N(1) = 2.14 (2) Å and Os(2)–N(2) = 2.11 (3) Å. The N(1)–N(2) distance of 1.20 (4) Å is consistent with that expected for an N=N double bond and may be compared with the N=N distance of 1.238 (18) Å in $(\mu\text{-H})Os_3(CO)_{10}(\mu\text{-}\eta^1\text{-N=N-}p\text{-}C_6H_4CH_3)$;[9] however, we must emphasize that the current structure is not of the highest accuracy and the esd on the N=N distance is rather large.

The dihedral angle between the trisomium plane and the Os(3)–N(1)–N(2)–Os(2) plane is 103.25°. (That between the Os(3)–N(1)–N(2)–Os(2) plane and the phenyl ring is

---

(28) (a) Churchill, M. R.; DeBoer, B. G.; Rotella, F. J. *Inorg. Chem.* **1976**, *15*, 1843–1853. (b) Churchill, M. R. *Adv. Chem. Ser.* **1978**, *No. 167*, 36.

(29) Shapley, J. R.; Samkoff, D. E.; Bueno, C.; Churchill, M. R. *Inorg. Chem.* **1982**, *21*, 634–639.

(30) Churchill, M. R.; DeBoer, B. G. *Inorg. Chem.* **1977**, *16*, 878.

15.76°.) Atoms N(1) and N(2) occupy axial sites on the cluster. However, the N=N distance of 1.20 (4) Å taken in conjunction with the Os(2)–Os(3) distance of 2.895 (2) Å necessitates some distortions within the $Os_3(CO)_{10}$ skeleton. Thus, the reduced angles Os(3)–Os(2)–N(2) = 64.4 (7)° and Os(2)–Os(3)–N(1) = 68.6 (7)° are accompanied by the enlarged angles Os(3)–Os(2)–C(21) = 108.3 (15)° and Os(2)–Os(3)–C(32) = 105.8 (11)°.

If we ignore the Os(2)–Os(3) linkage, there are three osmium atoms, each having an essentially octahedral stereochemistry. The octahedra centered at Os(2) and Os(3) are rotated contrafacially due to the μ-η^2-N=NPh ligand. All other distances and angles in the molecule are normal.

Experimental Section

$Os_3(CO)_{12}$,[31] $H_2Os_3(CO)_{10}$,[32] and $Os_3(CO)_{10}(NCCH_3)_2$[33] were prepared by the published procedures. Aniline (Baker) and *p*-fluoroaniline (Aldrich) were distilled prior to use; *p*-toluidine (Aldrich) was sublimed prior to use. The arenediazonium tetrafluoroborates were prepared by diazotizing the appropriate aniline with $NaNO_2$. ^{15}N was introduced at N_α with $Na^{15}NO_2$ (Merck). Solvents were reagent grade and were dried over molecular sieves before use. Although reactants and products were air stable, reactions were performed under an atmosphere of dry nitrogen, unless otherwise noted.

^1H NMR spectra were recorded on Varian EM-390 and JEOL FX-60 instruments, with Me_4Si as an internal reference. ^{13}C NMR spectra were recorded on a JEOL FX-60 spectrometer, with Me_4Si as an internal reference. ^{19}F NMR spectra were recorded on a JEOL FX-60 instrument, with C_6H_5F as an internal reference. ^{15}N NMR spectra were recorded by Dr. Steve Ulrich on a Varian XL-100 spectrometer, with $Na^{15}NO_2/D_2O$ as an external reference. ^{15}N chemical shifts were subsequently converted to the $\delta(^{15}NH_3) = 0.0$ scale,[21] with $\delta(^{15}NO_2^-) = 608$.[34] UV–vis spectra were recorded on a Cary 14 spectrophotometer. IR spectra were recorded on Perkin-Elmer 599B and 281B instruments and werre calibrated with cyclohexane (ν_{CO}) and polystyrene (ν_{CO} and $\nu_{N=N}$). Mass spectra were obtained on a Varian-MAT CH-5 mass spectrometer in the Mass Spectrometry Laboratory at the University of Illinois. Elemental analyses were performed by the Microanalytical Laboratory of the School of Chemical Sciences at the University of Illinois.

Synthetic photolyses were carried out by using a 450-W medium-pressure mercury-vapor lamp (Ace-Hanovia) filtered only by the Pyrex reaction vessels. Quantum yields were determined by ferrioxalate actinometry.[35] Conversions were low (7 ± 2%) and were monitored by hydride signal intensity (vide infra). Samples in degassed *n*-heptane solutions were irradiated in sealed 5-mm NMR tubes. Filter solutions for isolating 313- and 366-nm light were contained in concentric cylindrical compartments between the lamp and the samples.[36] For 313-nm light, the inner compartment had a 1.0-cm path length and contained 1.8 M $NiSO_4$ and 5 g/L $KHC_8H_4O_4$ in water; the outer compartment had a path length of 2.0 cm and contained 1.6 M $NiSO_4$ and 0.75 M $CoSO_4$ in water. For 366-nm light, the inner compartment had a path length of 2.0 cm and contained 0.12 M $NiSO_4$ and 0.50 M $CoSO_4$ in water; the outer compartment had a path length of 1.0 cm and contained 6.4×10^{-4} M 3,7-dimethyl-3,6-diazacyclohepta-1,6-dienyl perchlorate in water.[37] Typical light intensities were 1.7×10^{-10} einstein/s at 313 nm and 4.9×10^{-9} einstein/s at 366 nm.

Syntheses of $HOs_3(CO)_{10}(\eta^1$-N=NAr). Ar = Ph. $H_2Os_3(CO)_{10}$ (50.3 mg, 0.0589 mmol) and $PhN_2^+BF_4^-$ (65.8 mg, 0.342 mmol) were stirred together in dichloromethane at 40 °C for 10 h, during which time the color of the solution changed from purple to green. After cooling, brief treatment with dry $NH_3(g)$ turned the solution yellow and precipitated $NH_4^+BF_4^-$. The supernatant was decanted, and the solvent was removed from it by rotary evaporation. Preparative TLC (petroleum ether/silica gel) of the residue followed by crystallization from dichloromethane/pentane gave the product as orange crystals (39.5 mg, 0.0413 mmol, 70.0%): IR (cyclohexane) ν_{CO} 2106 m, 2069 vs, 2059 s, 2024 vs, 2015, s 2003 vs, 1980 w, 1955 w cm^{-1}; ^1H NMR ($CDCl_3$) δ 6.8–7.5 (m, 5 H), −14.46 (s, 1 H); mass spectrum, *m/z* 962 (M^+, ^{192}Os), plus $(M - xCO)^+$ (x = 1–10).

Anal. Calcd for $C_{16}H_6N_2O_{10}Os_3$: C, 20.08; H, 0.63; N, 2.93. Found: C, 20.22; H, 0.65; N, 2.90.

Ar = *p*-$C_6H_4CH_3$. $H_2Os_3(CO)_{10}$ (47.8 mg, 0.0561 mmol) and *p*-$CH_3C_6H_4N_2^+BF_4^-$ (31.0 mg, 0.150 mmol) were stirred together in dichloromethane at 40 °C for 6 h. During this time, the same color change as described above was observed. Workup of the reaction mixture as above produced 43.2 mg (0.0445 mmol, 79.4%) of orange crystals: IR (cyclohexane) ν_{CO} 2106 m, 2066 vs, 2057 s, 2021 vs, 2013 s, 2000 vs, 1983 m, 1965 w, 1953 w cm^{-1}; ^1H NMR ($CDCl_3$) δ 7.49 (d, 2 H_a), 7.55 (d, 2 H_b) (J_{ab} = 9.0 Hz), 2.44 (s, 3 H), −14.36 (s, 1 H); $^{13}\{^1H\}$ NMR ($CDCl_3$) δ 180.3 (1 C), 176.7 (1 C), 176.2 (1 C), 175.2 (1 C), 171.9 (1 C), 171.5 (1 C), 170.2 (1 C), 168.4 (1 C), 165.0 (1 C), 164.6 (1 C); mass spectrum, *m/z* 976 (M^+, ^{192}Os), plus $(M - xCO)^+$ (x = 1–10).

Anal. Calcd for $C_{17}H_8N_2O_{10}Os_3$: C, 21.04; H, 0.83; N, 2.89. Found: C, 21.91; H, 0.94; N, 2.90.

Ar = *p*-C_6H_4F. $H_2Os_3(CO)_{10}$ (52.8 mg, 0.0677 mmol) and *p*-F–$C_6H_4N_2^+BF_4^-$ (29.3 mg, 0.139 mmol) were stirred together in dichloromethane at 40 °C for 15 h, during which time the same color change as described above occurred. Workup of the reaction mixture as above gave 31.1 mg (0.0400 mmol, 59.1%) of orange crystals: IR (cyclohexane) ν_{CO} 2108 m, 2071 vs, 2059 s, 2025 vs, 2012 s, 2004 vs, 1991 m, 1972 w, 1961 w cm^{-1}; ^1H NMR ($CDCl_3$) δ 6.91–6.45 (AB portion of ABX, 4 H) (J_{ab} = 9.3 Hz, J_{H_aF} = 10.5 Hz, J_{H_bF} = 5.4 Hz), −14.43 (s, 1 H); mass spectrum, *m/z* 980 (M^+, ^{192}Os), plus $(M - xCO)^+$ (x = 1–10).

Anal. Calcd for $C_{16}H_5FN_2O_{10}Os_3$: C, 19.72; H, 0.51; N, 2.87. Found: C, 19.78; H, 0.54; N, 3.32.

Synthesis of $HOs_3(CO)_{10}(\eta^2$-N=NAr) by Photolysis of $HOs_3(CO)_{10}(\eta^1$-N=NAr). In general, no attempt was made to carry synthetic photolyses to maximum conversion (vide infra). Synthetic photolyses were carried out in Pyrex round-bottom flasks. Compounds **1** were dissolved in *n*-heptane, and the solutions were purged with CO for 30 min. The flasks were then closed under CO with septum stoppers, so as to maintain CO atmospheres during the irradiations. Irradiation times were generally 4–6 h to obtain synthetically useful conversions. Mixtures of products and unreacted starting materials were separated by preparative TLC (petroleum either/silica gel), and $HOs_3(CO)_{10}(\eta^2$-N=NPh) and $HOs_3(CO)_{10}(\eta^2$-N=N-*p*-$C_6H_4F)$ were obtained as brown crystals from dichloromethane/pentane. $HOs_3(CO)_{10}(\eta^2$-N=N-*p*-$C_6H_4CH_3)$ was obtained as brown crystals from pentane.

Ar = Ph: IR (cyclohexane) ν_{CO} 2112 m, 2068 vs, 2063 (sh), 2030 s, 2022 s, 2006 s, 1998 m, 1990 m cm^{-1}; ^1H NMR ($CDCl_3$) δ 7.5 (br, 5 H), −13.48 (s, 1 H); $^{13}C\{^1H\}$ NMR ($CDCl_3$) δ 183.0 (1 C), 181.5 (1 C), 178.1 (1 C), 176.9 (1 C), 175.6 (2 C), 175.1 (1 C), 174.0 (1 C), 173.6 (2 C).

Anal. Calcd for $C_{16}H_6N_2O_{10}Os_3$: C, 20.08; H, 0.63; N, 2.93. Found: C, 20.19; H, 0.66, N, 2.91.

Ar = *p*-$C_6H_4CH_3$: IR (cyclohexane) ν_{CO} 2109 m, 2066 vs, 2061 (sh), 2027 s, 2020 s, 2003 s, 1995 m, 1987 m cm^{-1}; ^1H NMR ($CDCl_3$) δ 7.46 (d, 2 H_a), 6.94 (d, 2 H_b) (J_{ab} = 9.6 Hz), 2.46 (s, 3 H), −13.3. (s, 1 H).

Anal. Calcd for $C_{17}H_8N_2O_{10}Os_3$: C, 21.04; H, 0.83; N, 2.89. Found: C, 21.52; H, 0.91; N, 3.12.

Ar = *p*-C_6H_4F: IR (cyclohexane) ν_{CO} 2109 m, 2066 vs. 2066 vs, 2058 s, 2027 s, 2014 s, 2007 m, 1997 w, 1989 w cm^{-1}; ^1H NMR ($CDCl_3$) δ 7.33–6.59 (AB portion of ABX, 4 H) (J_{ab} = 9.3 Hz, J_{H_aF} = 8.6 Hz, J_{H_bF} = 3.6 Hz), −13.42 (s, 1 H).

Anal. Calcd for $C_{16}H_5FN_2O_{10}Os_3$: C, 19.72; H, 0.51; N, 2.87. Found: C, 19.96; H, 0.54; N, 2.90.

Mass spectra were identical with those of the η^1 isomers.

Repeated Photochemical Thermal Cycling of $HOs_3(CO)_{10}(\eta^1$-N=N-*p*-$C_6H_4CH_3)$ and $HOs_3(CO)_{10}(\eta^2$-N=N-*p*-$C_6H_4CH_3)$. Two matched 15-mg samples of $HOs_3(CO)_{10}(\eta^1$-N=N-*p*-$C_6H_4CH_3)$ were placed in 5-mm NMR tubes and dissolved in *n*-heptane. The solutions were degassed by several freeze/pump/thaw cycles, and then the tubes were sealed under ca. 1 atm (25 °C) of CO. One tube was reserved as a control, subjected to neither irradiation nor pyrolysis, so that total hydride signal intensity could be monitored. The other tube was subjected to standard irradiation/pyrolysis cycles consisting of a 2.5-h

---

(31) Bradford, C. W.; Nyholm, R. S. *Chem. Commun.* **1967**, 384.

(32) Knox, S. A. P.; Koepke, J. W.; Andrews, M. A.; Kaesz, H. D. *J. Am. Chem. Soc.* **1975**, *97*, 3942.

(33) Tachikawa, M.; Shapley, J. R. *J. Organomet. Chem.* **1977**, *124*, C19.

(34) Lambert, J. B.; Roberts, J. D. *J. Am. Chem. Soc.* **1965**, *87*, 4087.

(35) Hatchard, C. G.; Parker, C. A. *Proc. R. Soc. London, Ser. A* **1956**, *235*, 518–36.

(36) Gard, D. R. Ph.D. Thesis, University of Illinois, Urbana, Illinois, 1981.

(37) Alway, D. G.; Barnett, K. W. Inorg. *Chem.* **1980**, *19*, 1533.

Table IV. Final Atomic Coordinates and Isotropic Thermal Parameters (Å^2) for (μ-H)$Os_3(CO)_{10}$(μ-η^2-N=NPh)

atom	x	y	z	B_{iso}
Os(1)	0.3591 (1)	0.1658 (1)	0.1963 (1)	
Os(2)	0.2709 (1)	0.0846 (1)	0.0515 (7)	
Os(3)	0.0737 (1)	0.0968 (1)	0.1769 (7)	
N1	0.144 (3)	−0.063 (2)	0.159 (2)	7.2 (9)
N2	0.227 (3)	−0.061 (2)	0.107 (1)	3.5 (6)
C(1)	0.272 (3)	−0.169 (3)	0.086 (2)	3.4 (6)
C(2)	0.341 (4)	−0.187 (4)	0.012 (2)	4.8 (8)
C(3)	0.386 (4)	−0.292 (4)	−0.010 (2)	4.7 (9)
C(4)	0.354 (6)	−0.375 (4)	0.041 (3)	6.9 (11)
C(5)	0.288 (5)	−0.358 (5)	0.122 (3)	7.2 (12)
C(6)	0.254 (5)	−0.253 (5)	0.139 (3)	6.5 (12)
C(11)	0.289 (4)	0.313 (4)	0.170 (3)	4.8 (8)
O(11)	0.256 (3)	0.396 (2)	0.153 (2)	
C(12)	0.411 (4)	0.011 (4)	0.223 (3)	5.0 (9)
O(12)	0.450 (3)	−0.065 (2)	0.231 (2)	
C(13)	0.356 (3)	0.209 (3)	0.305 (2)	3.5 (6)
O(13)	0.358 (3)	0.238 (3)	0.364 (1)	
C(14)	0.554 (3)	0.195 (3)	0.175 (2)	3.7 (7)
O(14)	0.665 (3)	0.225 (3)	0.159 (2)	
C(21)	0.305 (4)	0.234 (5)	0.012 (3)	5.2 (10)
O(21)	0.325 (4)	0.308 (2)	−0.005 (2)	
C(22)	0.187 (3)	0.037 (3)	−0.045 (2)	3.7 (7)
O(22)	0.140 (3)	0.024 (3)	−0.100 (2)	
C(23)	0.458 (4)	0.073 (3)	0.036 (2)	3.9 (7)
O(23)	0.574 (3)	0.035 (4)	0.013 (2)	
C(31)	0.072 (4)	0.080 (4)	0.284 (2)	4.2 (7)
O(31)	0.061 (3)	0.075 (3)	0.350 (2)	
C(32)	−0.004 (4)	0.252 (4)	0.176 (2)	4.0 (7)
O(32)	−0.044 (3)	0.327 (2)	0.178 (2)	7.6 (9)
C(33)	−0.110 (6)	0.047 (5)	0.156 (3)	7.4 (13)
O(33)	−0.216 (3)	0.002 (2)	0.153 (2)	

photolysis followed by a 2.5-h pyrolysis. The 2.5-h photolysis generated a mixture of ca. 40% **1** and ca. 60% **2**. The 2.5-h pyrolysis produced the "thermal" mixture of >95% **1** and <5% **2**. Ten such cycles produced cluster decomposition of less than 5%, as judged by ^1H NMR, although this treatment did cause some irreversible darkening of the solution.

Extent of Conversion of $HOs_3(CO)_{10}$(η^1-N=N-*p*-$C_6H_4CH_3$) to $HOs_3(CO)_{10}$(η^2-N=N-*p*-$C_6H_4CH_3$). The control tube from the previous experiment was photolyzed with periodic monitoring of the hydride-region ^1H NMR. Irradiation for 4.5 h produced a mixture of ca. 85% **2** and ca. 15% **1**. Further irradiation resulted in no further increase in the amount of **2** relative to **1**. Extensive further irradiation resulted in slow net cluster degradation.

Synthesis of $HOs_3(CO)_{10}$(η^2-N=NPh) from $Os_3(CO)_{10}(NCCH_3)_2$ and $PhNHNH_2$. $Os_3(CO)_{10}(NCCH_3)_2$ derived from 50.0 mg of $H_2Os_3(CO)_{10}$ (0.0586 mmol) was dissolved in dichloromethane, and $PhNHNH_2$ (2.8 μL, 1 equiv) was added by syringe. The solution immediately started to change color from yellow to orange; this color change appeared complete within ca. 30 min. The mixture was stirred at 25 °C for 30 min more, and then the solvent was removed by rotary evaporation. Preparative TLC (petroleum ether/silica gel) of the residue gave the major product as an orange band. Crystallization from dichloromethane/pentane gave 25.0 mg (0.0261 mmol, 44.6%) of brown crystals, which were analytically and spectroscopically identical with $HOs_3(CO)_{10}$(η^2-N=NPh) prepared by photolysis of $HOs_3(CO)_{10}$(η^1-N=NPh).

Collection of X-ray Diffraction Data for (μ-H)$Os_3(CO)_{10}$(μ-η^2-N=NPh). The obtention of crystals suitable for a single-crystal X-ray diffraction study was very difficult. All were very thin plates with a marked propensity for interpenetration twinning. The crystal eventually selected for the diffraction study had approximate dimensions of 0.3 × 0.1 × 0.02 mm. It was sealed under Ar in a 0.1-mm-diameter capillary and mounted (with its extended direction coincident with the diffractometer's ϕ axis) on our Syntex $P2_1$ automated four-circle diffractometer. Data were collected as described previously;[38] details are given in Table III. All data were converted to $|F_o|$ values following correction were performed on the SUNY—Buffalo-modified Syntex XTL in-house structure-solving system. The structure was solved by a combination of Patterson, difference-Fourier, and full-matrix least-squares refinement techniques. At convergence, discrepancy indices[39] were $R_F = 7.7\%$, $R_{wF} = 7.4\%$ and GOF = 1.99 for 185 parameters refined against 2114 independent data. (Os and O atoms were refined anisotropically; N and C atoms, isotropically.)

Since the space group is noncentrosymmetric, atoms were inverted ($x, y, z \rightarrow 1 - x, 1 - z$) and the structure refined to convergence once more. The discrepancy indices thus obtained were slightly higher than the previous values, so the original choice defined the correct enantiomorph; these later results were discarded.

The analytical forms of the scattering factors of neutral atoms[40a] were corrected for both the $\Delta f'$ and $i\Delta f''$ terms.[40b] The function minimized was $\sum w(|F_o| - |F_c|)^2$ with $w = [(\sigma(|F_o|))^2 + 0.02|F_o|^2]^{-1}$. Final parameters are listed in Table IV.

Acknowledgment. This work was supported by the National Science Foundation (Grants CHE 81-00140 to J.R.S. and CHE 80-23448 to M.R.C.).

Registry No. **1** (Ar = Ph), 88200-48-0; **1** (Ar = *p*-$C_6H_4CH_3$), 76756-17-7; **1** (Ar = *p*-C_6H_4F), 88200-49-1; **2** (Ar = Ph), 88200-50-4; **2** (Ar = *p*-$C_6H_4CH_3$), 88200-51-5; **2** (Ar = *p*-C_6H_4F), 88200-52-6; $H_2Os_3(CO)_{10}$, 41766-80-7; $Os_3(CO)_{10}(NCCH_3)_2$, 61817-93-4; $PhNHNH_2$, 100-63-0; $PhN_2^+BF_4^-$, 369-57-3; *p*-$C_6H_4FN_2^+BF_4^-$, 459-45-0; *p*-$C_6H_4CH_3N_2^+BF_4^-$, 459-44-9.

Supplementary Material Available: Lists of observed and calculated structure factor amplitudes, anisotropic thermal parameters, and least-squares planes for (μ-H)$Os_3(CO)_{10}$(μ-η^2-N=NPh) (15 pages). Ordering information is given on any current masthead page.

---

(38) Churchill, M. R.; Lashewycz, R. A.; Rotella, F. J. *Inorg. Chem.* **1977**, *16*, 265–271.

(39) $R_F = (\sum ||F_o| - |F_c|| / \sum |F_o|) \times 100$ (%); $R_{wF} = [\sum w(|F_o| - |F_c|)^2 / \sum w|F_o|^2]^{1/2} \times 100$ (%); GOF = $[\sum w(|F_o| - |F_c|)^2/(NO - NV)]^{1/2}$, where NO = number of observations and NV = number of variables.

(40) "International Tables for X-Ray Crystallography"; Kynoch Press: Birmingham, England, 1974; Vol. 4: (a) pp 99–101; (b) pp 149–150.